Chapter 5
Constructal Pattern Formation in Nature, Pedestrian Motion, and Epidemics Propagation

Antonio F. Miguel

5.1. Introduction

The emergence of shape and structure in animate and inanimate systems is among the most fascinating phenomena in our planet. Rivers carry water and sediment supplied by the hydrological cycle and erosional mechanisms, which play a major role in the shaping of the Earth's surface. River basins result, for instance, from these naturally organized flow architectures (Bejan 1999; Reis 2006a). Flow architectures also underline the phenomenon by which wet soil exposed to the sun and wind loses moisture, shrinks superficially, and develops a network of cracks (Bejan 2000). Similarly, in complex cellular systems such as the vertebrates, the requirement of large amount of oxygen for the metabolic needs of the cells constitutes the basis of the development of specialized and hierarchically organized flow systems, such as the respiratory tract and the circulatory system (Bejan et al. 2004; Reis et al. 2004; Bejan 2005; Reis and Miguel 2006).

The formation of dissimilar patterns inside similar systems under different environmental conditions is especially intriguing. Examples of these phenomena can be found in almost every field, ranging from physics to the behavior of social groups. For instance, in a horizontal fluid layer that is confined between two plates, and which is heated from below to produce a fixed temperature difference, there is a critical Rayleigh number for which the fluid breaks off from its macroscopically motionless form and starts to present a roll configuration—the Rayleigh–Bénard convection (Gettling 1998; Bejan 2000). It is equally well known that stony corals collected from exposed growth sites, where higher water currents are found, present more spherical and compact shape than corals of the same species growing in sheltered sites, which display a thin-branched morphology (Kaandorp and Sloot 2001; Merks et al. 2003). Furthermore, bacterial colonies that have to cope with hostile environmental conditions have more branched growth forms than colonies of the same species from nutrient-rich environments (Ben-Jacob et al. 1995; Thar and Kühl 2005). In a similar manner, plant roots seem to be able to respond to localized regions of high

nutrient supply by proliferating or elongating root branches into the nutrient-rich patches (Robinson 1994; Hodge et al. 1999). Root systems in soil are more open and more thinly branched than roots which are growing in hydroponics regime.

Pedestrian crowd motion also exhibits a variety of conjunction patterns, from more-or-less 'chaotic' appearance (Schweitzer 1997) to spontaneous organization in lanes of uniform walking direction looking like river-like streams (Navin and Wheeler 1969; Helbing et al. 2001). What determines the condition for the existence of so dissimilar patterns? Understanding crowd motion is essential on a wide range of applications including crowd safety (Donald and Canter 1990; Langston et al. 2006). From what principle can pedestrian facilities be deduced?

There has been a renewed impetus for the study of geotemporal spread of epidemics, following concerns over the increasing potential outbreak of infectious diseases (Koopmans et al. 2004; Hsu et al. 2006; Suwandono et al. 2006). Throughout history several pandemics have occurred in many areas of our planet, infecting and wiping out a large number of people. One of the most catastrophic pandemics was the bubonic plague (Black Death) in the fourteenth century. It is estimated that a third of the European population at the time died as a consequence of this outbreak. Moreover, historic records of the progress of this outbreak suggest a wave-like propagation of the disease (Langer 1964). What are the conditions for the existence of such a traveling wave? Would pandemics nowadays follow a similar propagation pattern as those that occurred in the fourteenth century?

In this chapter, we will examine the formation of dissimilar patterns inside similar systems from the viewpoint of the constructal theory of organization in nature (Bejan 1997, 2000; Bejan et al. 2004, 2006; Rosa et al. 2004; Bejan and Lorente 2005; Reis 2006b). Based on this view, common features between systems in very different fields are evidenced, and the importance of an optimum balance of competing trends (flow regimes, resistances, etc.) on the generation of patterns (architecture) is stressed. In particular, we aim to provide an answer to a very fundamental question: Have their patterns (architecture) in nature been developed by chance, or do they represent the optimum structure serving an ultimate purpose?

5.2. Constructal Law and the Generation of Configuration

Constructal theory is about the physics principle from which geometric form in flow systems can be deduced (Bejan 2000). Consider, e.g., the drainage of fluid through a nonhomogeneous surface (e.g., a surface with a central strip having a low resistance to fluid flow and lateral strips with high resistances to fluid flow) depicted in Fig. 5.1. According to the constructal law put forward by Bejan (1997, 2000), in order "for a flow system to persist (to survive) it must morph over time (evolve) in such a way that it provides easier access to the imposed currents that flow through it." Thus, the shape and flow architecture of

FIGURE 5.1. A surface with a central strip having a low resistance to fluid flow surrounded by strips with high resistance to fluid flow

the system in Fig. 5.1 do not develop by chance. In fact, the constructal theory proposes that every flow system exists with a purpose and that flows are free to morph their configuration in search of the best architectural solution within a framework of existing constraints (area or volume allocated, material properties, etc.). Therefore, the shape and flow architecture of the system are the result of the optimum balance between two competing trends—slow and fast (a surface with different flow resistances in this example, although it could be different flow regimes or other)—that ensures the maximization of fluid drainage.

In summary, the optimum balance between competing trends—slow (high resistivity) and fast (low resistivity)—is at the origin of shape and flow architecture.

5.3. Constructal Pattern Formation in Nature

5.3.1. Formation of Dissimilar Patterns Inside Flow Systems

The spreading of a tracer or a solute, and the transport of heat or fluid can be analyzed within the framework of diffusive–convective phenomena (Fig. 5.2). For example, the one-dimensional tracer transport within a fluid is governed by the macroscopic equation:

$$\frac{\partial n}{\partial t} + u\frac{\partial n}{\partial z} = D\frac{\partial^2 n}{\partial z^2} \tag{5.1}$$

where u is the average fluid velocity, D is the tracer diffusion coefficient, n is the tracer concentration, and t is the time. The time scales can be obtained by applying scale analysis (Bejan 2000) to the above equation:

$$\frac{\Delta n}{t} \sim D\frac{\Delta n}{L^2}, u\frac{\Delta n}{L} \tag{5.2}$$

Therefore, the characteristic times corresponding to the diffusive and convective driven transport are

$$t_{dif} \sim \frac{L^2}{D} \tag{5.3}$$

$$t_{cv} \sim \frac{L}{u} \tag{5.4}$$

FIGURE 5.2. The spreading of ink within water (slow or high resistivity) and boiling water (fast or low resistivity)

while the velocities are

$$v_{dif} = \frac{dL_{dif}}{dt} \sim \frac{1}{2}\left(\frac{D}{t}\right)^{1/2} \tag{5.5}$$

$$v_{cv} = \frac{dL_{cov}}{dt} \sim u \tag{5.6}$$

where t_{dif} and t_{cv} are the characteristic times corresponding to diffusive and convective driven transport, and v_{dif} and v_{cv} are the velocities corresponding to diffusive and convective driven transport, respectively.

The transition time from diffusive to convective driven transport, t^*, is obtained from the intersection of Eqs. (5.3) and (5.4):

$$t^* = \frac{D}{u^2} \tag{5.7}$$

If $t < t^*$ diffusion overcomes convection. Conversely, when $t > t^*$ tracer transport is mainly driven by convection.

Diffusion coefficients are usually much smaller than $1\,m^2s^{-1}$ (e.g., the diffusion coefficient for oxygen in air is approximately $2 \times 10^{-5}\,m^2s^{-1}$). When $u << D$ (e.g., u is close to zero), the time of transition t^* becomes very large ($t^* \to \infty$). In this situation, transition from diffusive to convective driven transport is not very likely to occur and the tracer transport is linked only to a diffusive phenomenon. However, if fluid velocity is much larger than the tracer diffusivity, the transition time (Eq. 5.7) is very small. What are the consequences of this? The initial diffusive velocity (Eq. 5.5) is larger than any convective velocity

(Eq. 5.6), but decreases as $t^{-1/2}$. Diffusion is the main driving mechanism at very beginning of the transport process but for times slightly greater than t^*, convective transport takes its place as the main mechanism. Similar results were obtained by Bégué and Lorente (2006) for the ionic transport through saturated porous media.

In summary, the architecture of the flow is the result of the trade-off between two competing trends—diffusion (slow or high resistivity) and convection or channeling (fast or low resistivity)—which ensure the maximization of the transport process.

Other flow systems exhibit a similar tendency. Bejan (2000) showed that the onset of a roll configuration in fluid layers heated from below (Rayleigh-Bénard convection) can be predicted based on the constructal theory. Conduction or thermal diffusion (high resistivity) prevails as the main mechanism, as long as it provides the shortest time in transporting heat across a surface layer. Conversely, rolls/channeling or convection cells (low resistivity) start to occur when the Rayleigh number reaches a critical value (>1700), so as to maximize the heat transport process (Fig. 5.3). Therefore, flow architecture is the result of the trade-off between two competing trends, and rolls are the optimized access for internal currents (e.g., the optimal architecture). Bejan (2000) also showed that a turbulent flow is a combination of the same two mechanisms—viscous diffusion (high resistivity) and eddies (low resistivity)—and can therefore be covered by the constructal law.

5.3.2. The Shapes of Stony Coral Colonies and Plant Roots

In stony corals and other organisms, which have a relatively weakly developed transport system, the amount of nutrients arriving at a certain site in the tissue, as well as the local deposition velocity of the skeleton material, are limited both by the locally available suspended material and the local amount of contact with the environment (Sebens et al. 1997; Anthony 1999). In plants, the water and dissolved minerals necessary for their survival are provided by the

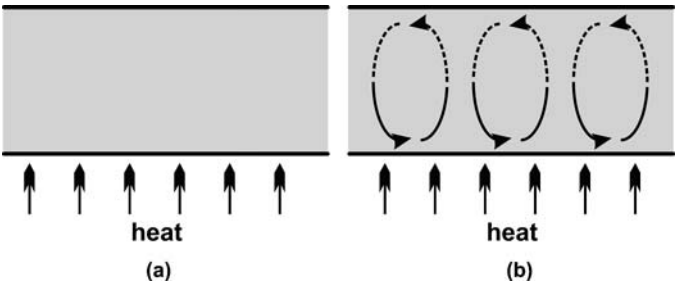

FIGURE 5.3. Rayleigh–Bénard convection: the fluid layer remains macroscopically motionless (a) but after the critical Rayleigh number the fluid presents a roll configuration (b)

root systems. Consequently, plants produce new roots to maximize nutrient absorption and continue to grow.

Both coral colonies and plant roots show an intraspecific variability of the shape. They may develop a branched or a more round shape apparently in a differentiated response to the variability of environmental conditions (Thaler and Pages 1998; Merks et al. 2003). For example, it is known that stony corals collected from exposed growth sites, where higher water currents are found, present more spherical and compact shape, than corals of same species from sheltered sites, which display more thin-branched morphologies (Merks et al. 2003).

Branched and circular (round) shapes are quite different regarding their ability to fill space (Fig. 5.4). Consider that l is the characteristic length/radius of the biological system and w is the width of the branch/needle (e.g., a very small quantity). The surface area of the biological system is $\sim lw$ for branches/needles and $\sim l^2$ for a circular shape. Undoubtedly, $l^2 >> lw$ which means that the circular shape is the most effective arrangement for filling the space in the shortest time and thus, according to the constructal law, it constitutes the optimal architecture. But sometimes stony corals and roots develop a branched shape. How can one reconcile such an obvious contradiction with the maximization of flow access?

The answer was provided by Miguel (2004, 2006), based on the constructal description made by Bejan (2000) of the structure of a dendritic crystal formed during rapid solidification. Consider, e.g., stony corals growing in exposed (open) sites. In this case, nutrient transport is driven mainly by convection. The velocity of the nutrient-rich water which surrounds the coral colony is much larger than the growth velocity of corals (which for a specie named *Porites* spp. is, for instance, about 12 mm per year). This implies that the coral grows always inside a region where nutrients are readily available. Consequently, it is able to spread (diffuse) in all directions and develop the most effective arrangement for filling the space in the shortest time—a round shape.

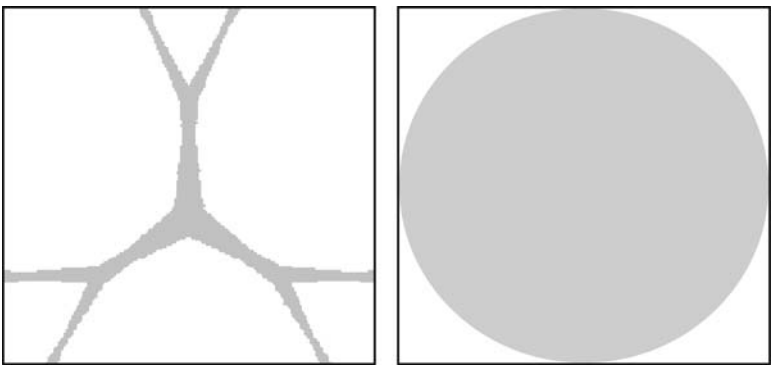

FIGURE 5.4. Branched and circular shape geometries and their ability to fill the space

Assume that the coral is growing in a sheltered site. When the velocity of the water containing nutrients becomes close to zero, the transport of nutrients is mainly due to diffusion and nutrients close to the coral colony are quickly depleted. Thus, the decrease of nutrient concentration around the coral triggers a wave of nutrients with a velocity of propagation $v_{dif} = \frac{dL_{dif}}{dt} \sim \frac{1}{2}\left(\frac{D}{t}\right)^{1/2}$, Eq. (5.5), and a characteristic length $L_{dif} \sim \frac{1}{2}(Dt)^{1/2}$. The initial velocity of propagation $v_{dif} \to \infty$ is much larger than the growth velocity of corals (~ 12 mm per year), but decreases as $t^{-1/2}$. Thus, there is a moment when the growth speed of the biological system exceeds the speed of nutrient propagation.

The temporal evolution of the characteristic length of the coral and nutrient propagation are presented in Fig. 5.5. This plot shows that at the critical time, t_{ct}, the characteristic length of the coral system overtakes the characteristic length corresponding to the diffusive transport. From this moment on the circular shape is no longer the most effective arrangement to fill the space. At times slightly larger than t_{ct}, the biological system starts to grow outside of the nutrient diffusion region. Guaranteed survival, branches are then generated to promote the easiest possible access to nutrients. This "biological channeling" enables the system to experience again growth inside the nutrient diffusion region from t_{ct} until $2t_{ct}$. At times slightly greater than $2t_{ct}$, the coral once again sticks out the nutrient diffusion region. New branches are consequently sent forward in order to promote the growth inside the nutrient diffusion region until a new critical time is reached. This means that each branch generates a new group of branches, and the result of this process is a dendritic-shaped system. Thus, in these circumstances "biological channeling" clearly becomes the most competitive shape configuration.

To conclude, the coral system, in its struggle for survival, must morph toward the configuration that provides an easier access to nutrients. The generation of branches is the response of the system when growth takes it out of the nutrient-rich region. These branches provide thus the paths that maximize the access to nutrients (e.g., the branches constitute the optimal shape under these circumstances).

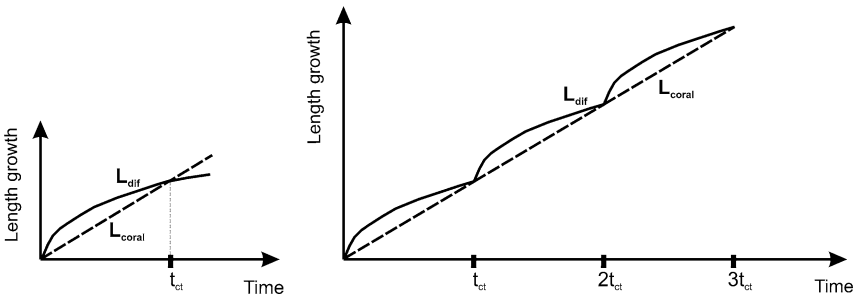

FIGURE 5.5. Simultaneous growth of characteristic lengths L_{coral} and L_{dif} and the occurrence of critical times t_{ct}

It is interesting to note that the optimal architecture of the system composed by nutrients and coral colony once more results from two competing trends: a convective (or channeling) transport of nutrients (e.g., low resistivity) implies a round (diffusive) coral morphology (e.g., high resistivity), while a diffusive (round) transport of nutrients (e.g., high resistivity) implies a branched (channeling) coral morphology (e.g., low resistivity). Similar results are also achieved for plant roots (Miguel 2006).

5.4. Constructal Patterns Formation in Pedestrian Motion

5.4.1. Pedestrian Dynamics: Observation and Models

The interest in the movement of crowds is not a recent one: it has existed ever since large events involving high number of people were organized. Roman amphitheatres, e.g., were built in such a way as to ease the entrance or exit of the venue for spectators. The Coliseum in Rome, for instance, has 80 strategic walkways designed to facilitate access and exit.

Pedestrian dynamics has an important impact on a wide range of applications including transportation (Timmermans et al. 1992; Hankin and Wright 1958), architecture and urban planning (Thompson and Marchant 1995), event organization (Smith and Dickie 1993), emergency exit planning (Donald and Canter 1990, Langston et al. 2006), and crowd control (Hunter et al. 2005).

One is usually convinced that human behavior is unpredictable and the way that people move is chaotic or, at least, very irregular. However, during the last decades, the systematic observation of pedestrians conducted by different researchers (e.g., see Hankin and Wright 1958; Older 1968, Navin and Wheeler 1969; Fruin 1971; Henderson 1971; Helbing et al. 2001) revealed that, in standard situations, individuals employ an optimized behavioral strategy. These observations can be summarized as follows:

(i) As long as it is not essential to move faster in order to get to their destination in time (like, for instance, running to catch a departing bus), pedestrians prefer to progress at the least-energy consuming most comfortable walking velocity. This desired velocity is of about $1.34\,\mathrm{ms}^{-1}$ and a standard deviation of $0.26\,\mathrm{ms}^{-1}$.
(ii) Pedestrians can move freely only at low pedestrian densities. As the pedestrian density increases (e.g., interpersonal distances lessen), walking velocity decreases.
(iii) A group of pedestrians (families, friends, colleagues) behave similarly to single pedestrians (group sizes are Poisson distributed).
(iv) Pedestrians try to keep a certain distance between themselves or to borders (walls, objects, columns, etc.). This behavior helps to avoid contact in case of sudden velocity change and maintain a private area around (territorial effect).
(v) Pedestrians feel uncomfortable when they have to move in a direction opposite to the destination.

FIGURE 5.6. Pedestrians have a preferred side to walk that disappears at high pedestrian densities

(vi) Pedestrians have a preferred side to walk that disappears at high pedestrian densities (Fig. 5.6).
(vii) In general, pedestrians act more or less automatically, they do not reconsider their behavioral strategy when facing new situations.

It is interesting to note that the movement of pedestrians displays many of the attributes of fluid and granular* flows (Helbing et al. 2001, Hughes 2003):

(i) Footsteps in the sand and snow look similar to fluid streamlines (Fig. 5.7).
(ii) Pedestrians organize themselves in the shape of river-like streams (channeling) when a stationary crowd needs to be crossed (Fig. 5.8).
(iii) When moving in crowded places, individuals organize themselves spontaneously in lanes of uniform walking direction (channeling) (Fig. 5.9).
(iv) In dense crowds which push forward, one can observe a kind of shock-wave propagation.

FIGURE 5.7. Footsteps in the sand (a) and snow (b) look similar to fluid streamlines (c)

* Two-phase flow consisting of particulates and an interstitial fluid that when sheared the particulates may either flow in a manner similar to a fluid or resist the shearing like a solid.

FIGURE 5.8. Pedestrians organize themselves in the shape of river-like streams (channeling) when a stationary crowd needs to be crossed

FIGURE 5.9. In crowded spaces, individuals self-organize in lanes of uniform walking direction (channeling)

(v) At bottlenecks (e.g., doors, corridors) the pedestrian's passing direction oscillates with a frequency that increases with width and declines with the length of the bottleneck. This is similar to granular "ticking hour glasses," in which grains alternate between flowing and not flowing at a constant rate.

A number of empirical models based on observational data are available in published studies (e.g., see Predtechenskii and Milinski 1969; Sandahl and Percivall 1972; TRB 1985; Nelson and MacLennan 1995; Graat et al. 1999). Some models considering the analogies between physical systems and pedestrian motion have also been proposed, a number of which represent crowds as an aggregate of individuals having a set of motivations and basic rules (Table 5.1). The so-called social force model (Helbing 1992; Helbing and Molnár 1995) has its origins in gas-kinetic models and was developed to describe the dynamics of pedestrian crowds. It consists of self-driven people (particles) that interact through social rules—the "social forces." These forces produce changes in the velocities and reflect in turn, a change in motivation rather than in the physical forces acting on the person. The models presented by Hoogendoorn and

TABLE 5.1. Models for pedestrian motion

Authors	Characteristics	Validity
Blue and Adler (1999)	Cellular automata discrete model	Density less than five people per square meter
Fukui and Ishibashi (1999)	Cellular automata discrete model	–
Helbing (1992) Helbing and Molnár (1995)	Social force	High and low densities
Helbing et al. (1997)	Active walker	low density
Hoogendoorn and Bovy (2000) Hoogendoorn et al. (2002)	Extremal principle (generalization of the social force)	Density less than five people per square meter
Hughes (2002)	Thinking fluid	High and low densities
Langston et al. (2006)	Discrete element discrete model	High and low densities
Muramatsu et al. (1999)	Random walk	–

Bovy (2000) and Hoogendoorn et al. (2002) provide a generalization of the social force model. Early on, Reynolds (1987) presented a model to approach animal motion, like that of bird flocks and fish schools, that bears relevance to crowd dynamics. This flocking model consisted of three simple steering behaviors which described how each individual flocking element (called *boid*) maneuvered based on the positions and velocities of its nearby flock mates.

The "thinking fluid" model (Hughes 2002, 2003) results from the combination of fluid dynamics with three hypotheses which are supposed to govern the motion of pedestrians. These hypotheses, together with those governing the motion of the boids, and the "social forces" are listed in Table 5.2.

5.4.2. Diffusion and Channeling in Pedestrian Motion

The constructal law states that if a system is free to morph in time (evolve), the best flow architecture is the one that maximizes the global flow access (e.g., minimizes the global flow resistances). Thus, the shape and flow architecture of the system do not develop by chance, but result from the permanent struggle between slow and fast for better performance and must thus evolve in time (Bejan 2000).

How and by which mechanism do then pedestrians evolve in space and time? To answer this question, let us consider pedestrian groups that proceed from one point to every point of a finite-size area (territory). According to the constructal law, the best architecture will be the one that promotes the easiest flow of pedestrians. As described earlier, there are two mechanisms for achieving this purpose: diffusion (slow or high resistivity) and channeling (fast or low resistivity). The access time for a diffusive process through a territory of length L is $\sim L^2/D$, Eq. (5.3), and the access time for a channeling flow is $\sim L/u$, Eq. (5.4). To compare both times we need to know the pedestrian's diffusion coefficient, D, and the pedestrian's walking velocity, u.

TABLE 5.2. Hypotheses that support models describing the movement of individuals

Flocking model (Reynolds 1987)	Social forces model (Helbing and Molnár 1995)	"Thinking fluid" model (Hughes 2003)
• Boids try to fly toward the center of mass of neighboring boids • Boids try to keep a small distance away from other objects (including other boids) • Boids try to match velocity with near boids	• Pedestrians move as efficiently as possible to a destination • Pedestrians try to maintain a comfortable distance from other pedestrians and from obstacles like walls • Pedestrians may be attracted to other pedestrians (e.g., family, friends) or objects (e.g., posters, shop windows)	• Walking velocity is determined only by the density of surrounding pedestrians, the behavioral characteristics of the pedestrians, and the ground characteristics • Pedestrians at different locations but with same sense of the task (called potential) would see no advantage to exchanging places • Pedestrians minimize their estimated travel time but also try to avoid extreme densities

In accordance with field surveys, it has been established that pedestrians prefer to move with a walking velocity around $1.34\,\mathrm{ms}^{-1}$, which corresponds to the least energy-consuming velocity (Fruin 1971; Henderson 1971; Helbing et al. 2001). This walking velocity is only reachable if there are no other pedestrians and obstacles in the surroundings. Furthermore, it was noticed that pedestrians in a shopping mall or busy city street (random and nondirectional crowd) exhibit a velocity reduction that is related with the free area available around each individual (Fig. 5.10). Consequently, and as in physics, the pedestrian's diffusion coefficient may be defined as the product of walking (random) velocity, u_{crd}, and the mean available interpersonal distance, λ.

A pedestrian's diffusion coefficient—mean interpersonal distance relationship can be established with the help of the coefficient's definition and the data plotted in Fig. 5.10. This relationship is illustrated in Fig. 5.11. The form of the curve-fitted equation, justified by the correlation coefficient, is

$$D = a_1\lambda - a_2 \tag{5.8}$$

Here a_1 and a_2 are the correlation coefficients, which have been listed in Table 5.3. Consider, e.g., the curve-fitted equation obtained based on Fruin data (Fruin 1971), that when combined with Eqs. (5.3) and (5.4) leads to

$$t_{dif} \sim \frac{L^2}{1.61\lambda - 0.67} \qquad (0.48 \le \lambda \le 3.16) \tag{5.9}$$

$$t_{cv} \sim 0.75L \tag{5.10}$$

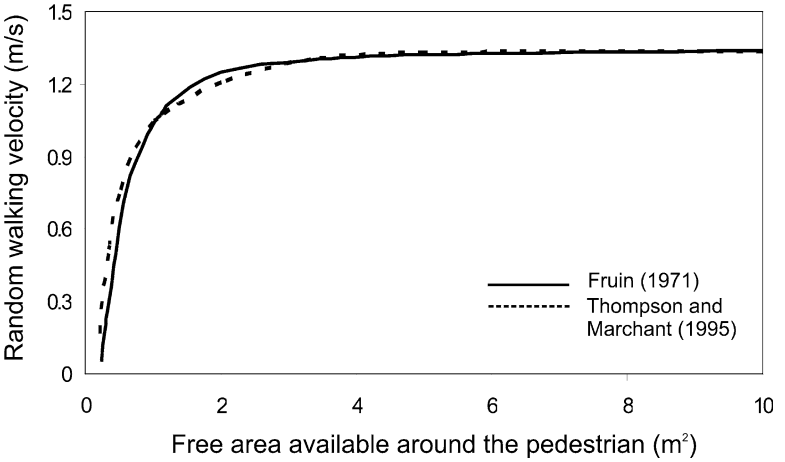

FIGURE 5.10. Effect of the free area available around the pedestrian on the random walking velocity

Based on this, it is straightforward to conclude that channeling enables a better performance if L/λ is larger than $1.2-0.5\,\lambda^{-1}$ (or in terms of the pedestrians' density, ρ, larger than $1.2-0.5\,\rho^{-1/2}$). Otherwise, diffusion becomes clearly the most competitive transport mechanism.

To summarize, there are two optimal modes of locomotion for pedestrians: channeling which is suitable to distribute pedestrian through a territory (area) and diffusion which becomes more appropriate when accessing space locally (e.g., access to train platforms and bus stops, buildings entrance, etc.). This finding has an impact on not only in the design of new pedestrian facilities but

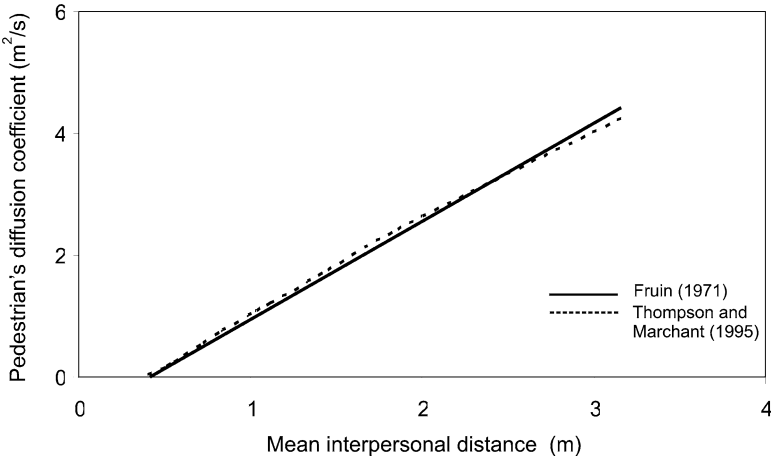

FIGURE 5.11. Pedestrian's diffusion coefficient versus the mean interpersonal distance

TABLE 5.3. Correlation coefficients for pedestrian's diffusion coefficient—mean interpersonal distance relationship

	a_1	a_2	r^2	Validity
Random crowd in a city street Fruin (1971)	1.61	0.67	0.992	$0.48 \leq \lambda \leq 3.16$
Random crowd in area of a building Thompson and Marchant (1995)	1.56	0.56	0.997	$0.40 \leq \lambda \leq 3.16$

also in the improvement of existing facilities. If the target is to promote the easiest access to pedestrians over a large territory where, for some reason, the velocity is lower than the desired walking velocity ($\sim 1.34\,ms^{-1}$), the placement of gates/lanes/columns/trees along walkways/corridors helps to stabilize the pedestrian flow and make it more fluid (Fig. 5.12). This channeling also allows pedestrians to keep a certain distance from other pedestrians which is highly appreciated (very small interpersonal distances induces contact "collisions" among pedestrians which is seen as "uncomfortable" (TRB, 1985)). The placement of gates/lanes/columns/trees (channeling) is especially important in case of pedestrians walking in opposite directions (Fig. 5.13).

Pedestrians have a preferred side to walk because they profit from it (e.g., moving against the stream is more difficult because it increases interaction and consequently the resistance). Therefore, a baffler along walkways/corridors helps to optimize the flow of pedestrians, as well as to save space that can be used for other purposes.

5.4.3. Crowd Density and Pedestrian Flow

Empirical observations have also highlighted that pedestrians can move freely only at very small pedestrian densities. Fig. 5.14 illustrates velocities of pedestrians in the crowds. Pedestrians in low-density crowds ($\rho < 1$ person m^{-2}) are able to walk with an individual desired velocity that corresponds to the comfortable walking velocity ($\sim 1.34\,ms^{-1}$). In higher crowd densities, interpersonal distances are lessened and the walking velocity is reduced, in order to

FIGURE 5.12. Gates and lanes along walkways help to stabilize the pedestrian flow and make it more fluid

FIGURE 5.13. Pedestrians walking in opposite directions in crowded spaces

keep a certain distance from other pedestrians and to avoid contact. Therefore, pedestrian motion can be summarized as follows:

$$u = u_0 \quad \text{for} \quad 0 \le \rho \le \rho_{ct} \tag{5.11}$$

$$u = u(\rho) \quad \text{for} \quad \rho_{ct} < \rho \le \rho_{max} \tag{5.12}$$

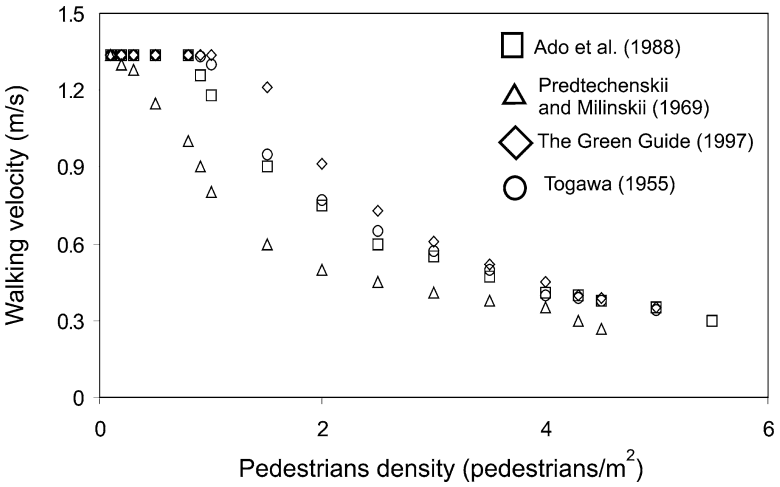

FIGURE 5.14. Walking velocities versus pedestrians' density

where u_0 is the desired velocity (e.g., $\sim 1.34\,ms^{-1}$), ρ_{ct} is the critical density of pedestrians (e.g., ~ 1 person m^{-2}) and ρ_{max} is the maximum density of pedestrians.

Let us suppose that, above the critical pedestrian density, the temporal change of the pedestrian velocity is the result of "repulsive" forces due to a decrease of interpersonal distances (especially the relative distance to the front person). "Repulsive" forces decrease with the interpersonal distance, and as the area available for the next step is accounted, they are also dependent of the walking velocity (Helbing et al. 2001). According to the Newton's second law of motion

$$\frac{d^2r}{dt^2} = F_r \tag{5.13}$$

Here r is the position of the pedestrian and F_r is the "repulsive" force per mass affecting the behavior of the pedestrian which is given by (Fang et al. 2003)

$$F_r = \frac{\gamma}{(r - r_o)}\left(\frac{dr}{dt} - \frac{dr_o}{dt}\right) \tag{5.14}$$

where γ is a constant, and $r - r_o (= \lambda)$ and $dr/dt - dr_o/dt$ are the mean interpersonal distance and the mean relative velocity to the pedestrians situated around, respectively. Replacing of F_r by Eq. (5.14) in Eq. (5.13) and integrating the resulting equation, we find that

$$u = \frac{dr}{dt} = \gamma \ln(\lambda) + c \tag{5.15}$$

where c is an integration constant. By definition, the interpersonal distance is minimum (e.g., crowd density maximum) when the walking velocity is zero. Thus, the constant c can be determined and Eq. (5.15) assumes the form

$$u = \gamma \ln\left(\frac{\lambda}{\lambda_{min}}\right) \tag{5.16}$$

and in terms of pedestrian density

$$u = \frac{1}{2}\gamma \ln\left(\frac{\rho_{max}}{\rho}\right) \tag{5.17}$$

In summary, Eqs. (5.16) and (5.17) should hold when the pedestrian's density is between the critical and the maximum densities. Note that experimental walking velocities in this density range show a good agreement with these equations (Fig. 5.15).

The flow of pedestrians may be defined as the product of walking velocity and pedestrian density,

$$\phi = \rho u \tag{5.18}$$

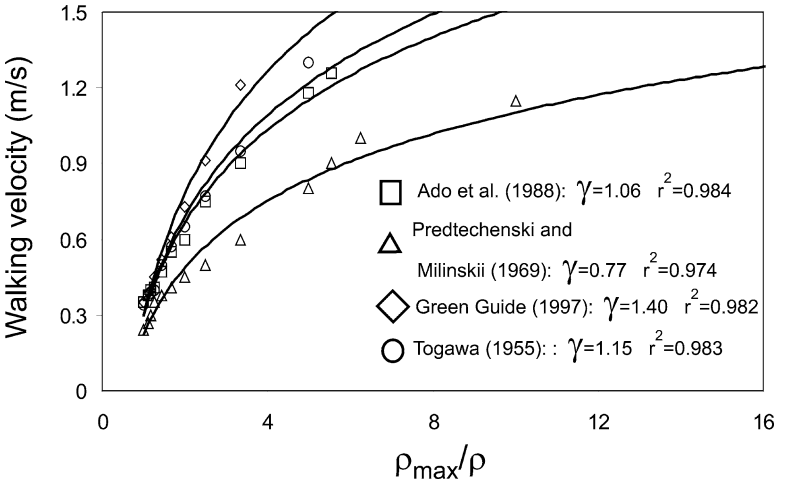

FIGURE 5.15. Experimental walking velocities and the fit with Eq. (5.17)

where ϕ is the pedestrian flow. Therefore, Eqs. (5.11), (5.12), (5.17), and (5.18) combine to form

$$\phi = \rho u_0 \quad \text{for} \quad 0 \le \rho \le \rho_{ct} \tag{5.19}$$

$$\phi = \frac{1}{2}\gamma \ln\left[\left(\frac{\rho_{max}}{\rho}\right)^{\rho}\right] \quad \text{for} \quad \rho_{ct} < \rho \le \rho_{max} \tag{5.20}$$

Based on these equations a flow–density diagram can be drawn (Fig. 5.16). When $\rho \le \rho_{ct}$, the individual desired velocity is a constant and the maximum flow of pedestrians corresponds to $\rho_{ct} u_0$. For densities above the critical density, there is also an optimal crowd density such that the flow of pedestrians is maximized. If we take Eq. (5.20), the flow has a maximum value of $0.5\gamma\rho_{max}/\exp(1)$ at $\rho = \rho_{max}/\exp(1)$. It is useful to obtain also the relationship between flow and velocity. For $\rho_{ct} < \rho \le \rho_{max}$ it follows from Eqs. (5.17) and (5.18) that

$$\phi = \rho_{max} \frac{u}{\exp(2u/\gamma)} \tag{5.21}$$

The flow–velocity diagram is depicted in Fig. 5.17. This diagram shows that there is also an optimal velocity such that the crowd flow is maximized. According to Eq. (5.21), the flow has a maximum value of $0.5\gamma\rho_{max}/\exp(1)$ at $u = \gamma/2$. As expected, this maximum flow has the same value as that obtained with Eq. (5.20).

Comparing the flow–density and flow–velocity diagrams (Figs. 5.16 and 5.17, respectively), we note that each velocity/density corresponds to a single flow but, with the exception of maximum flow, the same flow may correspond to two different velocities/densities. We can see how this behaviour can arise. As the

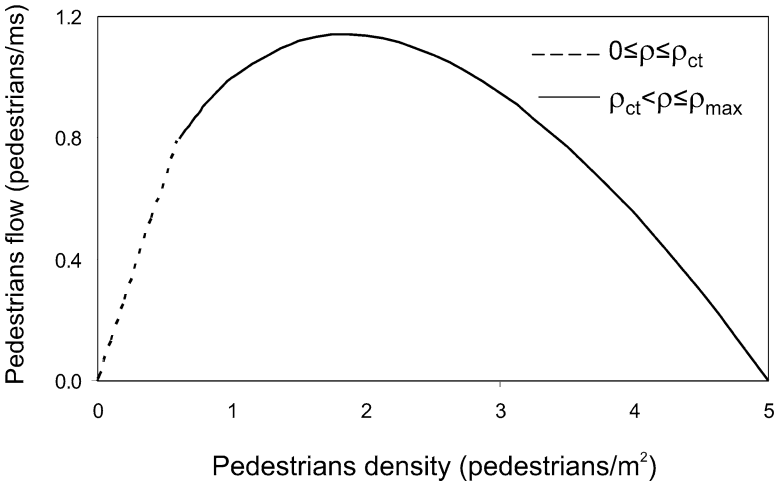

FIGURE 5.16. Flow–density diagram drawn with Eqs. (5.19) and (5.20) ($\rho_{max} = 5$ pedestrians per square meter)

flow progresses to the maximum, the increase of pedestrian velocity (or decrease of density) is offset by a decrease of pedestrian density (or increase of velocity). After reaching the maximum flow, there is a decrease of the pedestrian flow because the growth in velocity (or decrease of density) does not compensate the reduction of pedestrian density (or increase of velocity). Consequently, the same flow may correspond to two different velocities/densities.

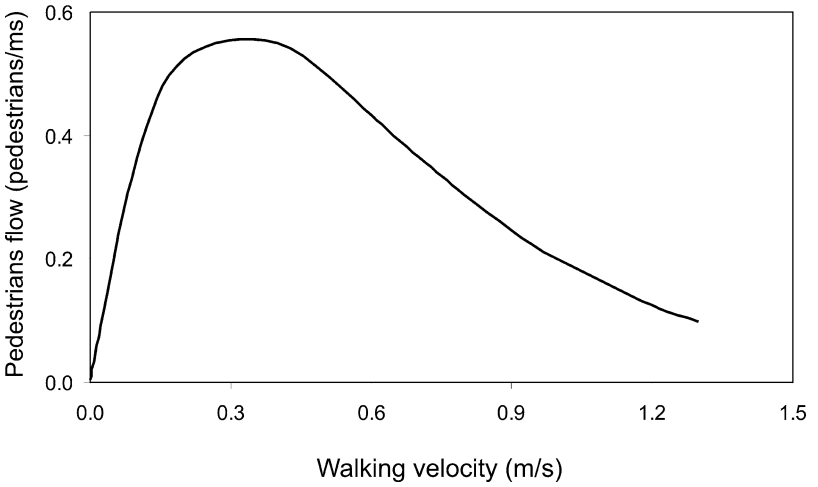

FIGURE 5.17. Flow–velocity diagram drawn with Eq. (5.21) ($\rho_{max} = 5$ pedestrians per square meter)

5.5. Optimizing Pedestrian Facilities by Minimizing Residence Time

5.5.1. The Optimal Gates Geometry

At high pedestrian densities, the walking velocity is drastically reduced and impatient pedestrians trying to use any gap to move on may lead in turn to a complete obstruction of walking paths. Thus, at a high density there is risk of overcrowding and personal injury that should be avoided.

Gates are used at sport facilities, theaters, and so on, to reduce the interpersonal interactions and stabilize the pedestrian flow, by facilitating the access over the territory (Fig. 5.12). Thus, pedestrians must be channeled optimally through gates since channeled flow is characterized by a much lower travel time (Section 5.4.2). The question put forward by the constructal principle is, then, how can the gates be designed in order to ensure that pedestrians flow over the entire space in the shortest time possible?

Consider a crowd approaching gates of the same size and uniformly distributed in space. According to mass conservation equation,

$$\rho u W_g = n \rho_i u_i w_g \tag{5.22}$$

where n is the number of gates, W_g is the total width allocated to the gates, w_g is the width of each individual gate, u is the velocity of the crowd approaching the gates, u_i is the pedestrians velocity within the gates, ρ is the density of the crowd approaching the gates, and ρ_i is the density of the pedestrians within the gates. The goal is the optimal spacing of the gates, w_g, in a fixed territory, W_g, to minimize the travel time of pedestrians defined as

$$t_{tr} = \frac{1}{l_g \phi} \tag{5.23}$$

Let us consider that the length of the gates, l_g, is fixed. The time of travel is minimal when the flow of pedestrians is maximal. It is not that difficult to show that the maximum flow of pedestrians corresponds to $0.5\gamma\rho_{max}/\exp(1)$ (Section 5.4.3) and that the minimum travel time is given by

$$t_{tr} = \frac{2\exp(1)}{l_g \gamma \rho_{max}} \tag{5.24}$$

Therefore, according to Eq. (5.22), nw_g/W_g is

$$\frac{nw_g}{W_g} = \frac{2\rho u \exp(1)}{\gamma \rho_{max}} \tag{5.25}$$

Recalling that flow ρu is given by Eq. (5.20), we can rewrite Eq. (5.25) in terms of the crowd density obtaining

$$\frac{nw_g}{W_g} = \frac{\rho}{\rho_{max}} \ln\left(\frac{\rho_{max}}{\rho}\right) \exp(1) \tag{5.26}$$

Given that ρ_{max} is a constant, the variation of nw_g/W_g is only dependent on the density of the crowd approaching the gates. Fig. 5.18 shows how nw_g/W_g responds to changes of crowd density. It reveals that there is a maximum for nw_g/W_g that occurs when $\rho/\rho_{max} \sim 0.37$. Thus, the optimal number of gates n is W_g/w_g taking $w_g \sim 0.75\,m$ which corresponds to the square root of the free area available around each individual when the flow of pedestrians is maximum (Fig. 5.16).

5.5.2. Optimal Architecture for Different Locomotion Velocities

Constructal theory also predicts the architecture of flow paths that connect a finite territory to a single point when different locomotion velocities are available (Bejan and Ledezma 1998; Bejan 2000). How should architects and urban planners design high performance path systems in these circumstances?

Let us assume that the territory is covered in sequential steps of increasingly larger elements ($A_1 < A_2 \ldots$). According to the constructal theory, the global system (territory) will perform best when all its elements (constructs, portions of territory) perform in an optimal way. Optimal geometry means elements (constructs) that minimize the travel time. Thus, both the shape of the area and the angle between each path and its branches are optimized at each stage. The flow path is constructed starting with the smallest element (construct, portions of territory) and continuing with the larger areas (assemblies, constructs).

Consider pedestrians walking in a rectangular domain with a fixed area $H_1L_1 (= A_1)$ at two different velocities: at velocity u_1 in all directions (diffusion) and at velocity u_2 along a centred longitudinal path ($u_1 < u_2$). The goal is

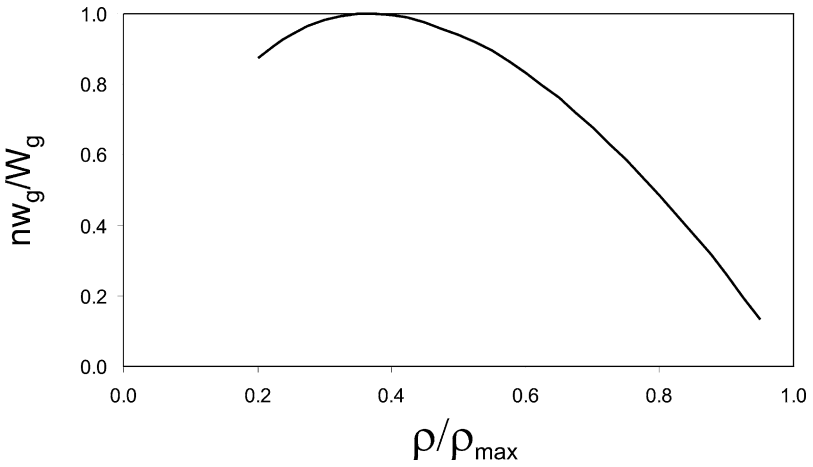

FIGURE 5.18. The variation of nw_g/W_g with respect to the density of the crowd approaching the gates

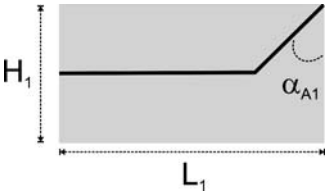

FIGURE 5.19. Rectangular domain with a fixed area H_1L_1 (adapted from Bejan 2000)

to minimize the travel time from anywhere within A_1 to an exit point at its periphery (Fig. 5.19). There are two degrees of freedom in this design: the shape H_1/L_1 and the deviation from the normal for the angle between the slower and the faster paths α_{A1}. Optimizing in view of the stated purpose delivers an optimal geometry and a characteristic travel time t_1 from the most distant point in A_1 until its exit point (Bejan and Ledezma 1998):

$$\left(\frac{H_1}{L_1}\right)_{\text{optimal}} = \frac{2}{\xi_1}\left(\frac{u_1}{u_2}\right) \tag{5.27}$$

$$(\alpha_{A1})_{\text{optimal}} = \cos^{-1}\xi_1 \tag{5.28}$$

$$t_1 = \left(\frac{2\xi_1 A_1}{u_1 u_2}\right)^{1/2} \tag{5.29}$$

with

$$\xi_1 = \left[1 - \left(\frac{u_1}{u_2}\right)^2\right]^{1/2} \tag{5.30}$$

This configuration also optimizes the access from the whole area to the same exit point (Bejan 2000). Consider now a larger fixed area $A_2(= H_2L_2)$ and a faster regime at velocity u_3 (e.g., the desired walking velocity) along a centred longitudinal path ($u_3 > u_2$). Once again one seeks to optimize the access from an arbitrary point of A_2 to a common exit point on its periphery. This problem can be addressed by filling A_2 with optimized A_1 areas, in a manner similar to the foregoing reasoning. The number of elements A_1 assembled into A_2 is given by

$$n_{A2A1} = 2\xi_1\xi_2\left(\frac{u_3}{u_1}\right)\left(1 - \frac{u_2^2}{4u_3^2}\right) \tag{5.31}$$

and the optimal geometry is represented by

$$\left(\frac{H_2}{L_2}\right)_{\text{optimal}} = \frac{1}{\xi_2}\left(\frac{u_2}{u_3}\right) \tag{5.32}$$

$$(\alpha_{A2})_{\text{optimal}} = \cos^{-1}\xi_2 \tag{5.33}$$

with

$$\xi_2 = \left[1 - \left(\frac{u_2}{2u_3}\right)^2\right]^{1/2} \tag{5.34}$$

These results are very similar to those obtained by the optimization of A_1 apart of a constant factor. This optimization can be repeated over larger areas, assemblies being the optimized configuration ratio given by relations similar to the ones obtained for A_2. The final paths' geometry forms a tree network.

Figures 5.20 and 5.21 show how the shape H/L and the optimal angle α_A respond to changes of velocity ratios. When the two modes of locomotion have similar velocities, the optimal angles α_{A1} and α_{A2} are close to 90° and 30°, respectively, and the optimal lengths H/L are maximal. On the other hand, if the faster walking velocity is much larger than the slower walking velocity then paths are perpendicular and the centred longitudinal path L is the much larger than H. We also note that H = L when $u_2/u_1 \sim 0.45$ ($\alpha_{A1} \sim 26.7°$) and $u_3/u_2 \sim 0.9(\alpha_{A2} \sim 26.7°)$.

5.5.3. The Optimal Queuing Flow

Another interesting collective effect of pedestrian dynamics is the formation of queues. Queuing is a common practice is our lives. One queues at the supermarket cashiers, at bus tops, at ticket offices, at stadium entrances, and so on. Once a queue is formed, it acquires dynamic of its own, attracting incomers in a forward motion.

Let q_a be the rate at which pedestrians with a velocity u_a arrive at a certain spot and q_s the rate at which they get served at that spot. When $q_s \geq q_a$, all

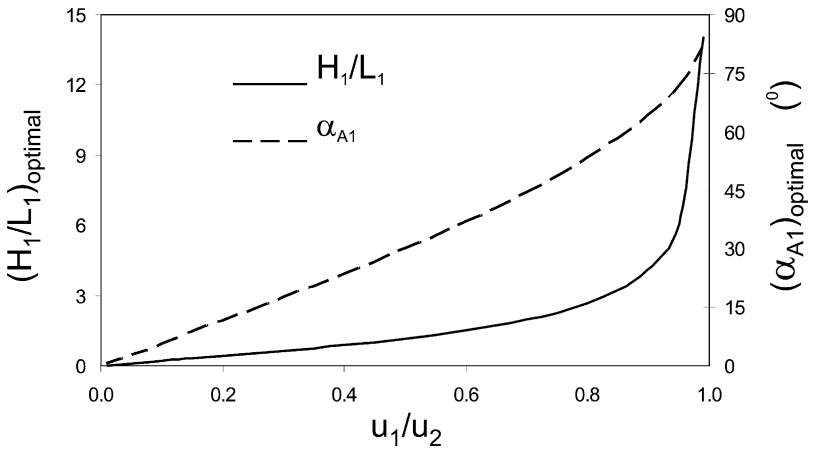

FIGURE 5.20. Optimal values of H_1/L_1 and α_{A1} versus u_1/u_2

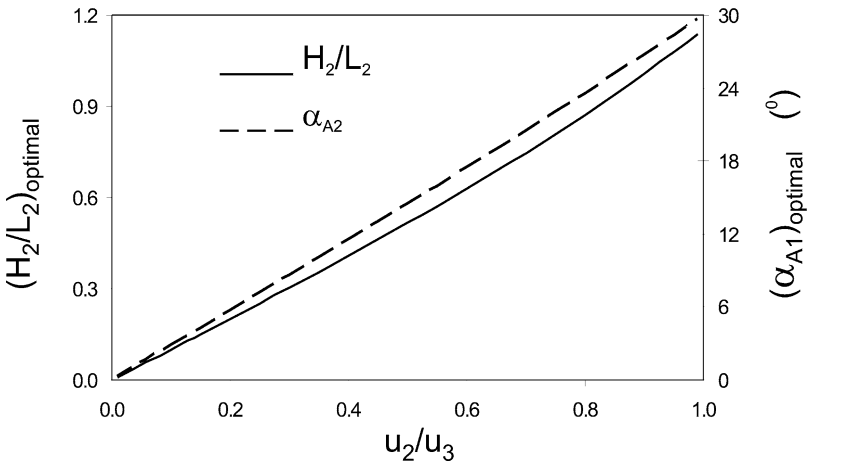

FIGURE 5.21. Optimal values of H_2/L_2 and α_{A2} versus u_2/u_3

individuals get served before queuing. Otherwise, there are individuals who need to wait in order to become served, which leads to the formation of a queue.

Empirical observations reveal that the higher the flow of individuals, the higher the queuing time. The velocity within the queue, v, is (Heidemann 1996; Vandaele et al. 2000)

$$v = 2u_a \frac{\rho_{max} - \rho}{2\rho_{max} + \rho\,(\beta^2 - 1)} \tag{5.35}$$

Here β is a coefficient that accounts for deviations from the expected service time (e.g., $\beta^2 = 1$ means that pedestrians are served within the expected time). The relation between velocity and flow in queues can be obtained by combining Eqs. (5.18) and (5.35) into

$$\phi = 2\rho_{max} v \frac{u_a - v}{2u_a + v\,(\beta^2 - 1)} \tag{5.36}$$

Based on this equation a flow–velocity diagram can be drawn (Fig. 5.22). This diagram reveals one flow can correspond to two different velocities (with the exception of the maximum flow) in spite of each pedestrian velocity matching a single pedestrian flow. This reasoning is analogous to the one put forward in Section 5.4.3.

Figure 5.22 also reveals that there is an optimal velocity such that the flow in the queue is maximized (or time of travel is minimized). When, for instance, $\beta^2 = 1$ the maximum flow is $u_a\rho_{max}/4$ and occurs when $v = u_a/2$. We can also observe that an increase of β^2 reduces the maximum value (the peak) of the flow and that this peak occurs at lower velocities. When $\beta^2 < 1$, the maximum flow occurs at higher velocities. After that the pedestrian flow drops very fast until it ceases totally. The reverse occurs if $\beta^2 > 1$. A straightforward explanation can

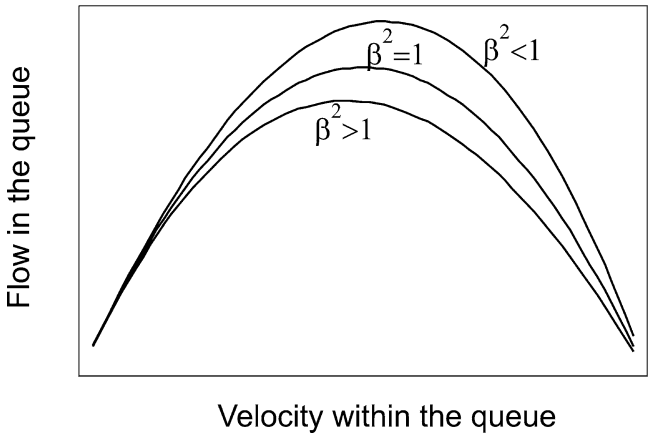

FIGURE 5.22. Flow-velocity diagram drawn with Eq. (5.36)

be provided for this finding. If β^2 is lower than 1, this means that pedestrians get served before the expected time. Consequently, more pedestrians are allowed to enter in the queue, which can be by increasing the arrival velocity of pedestrians to the queue.

5.6. Constructal View of Self-organized Pedestrian Movement

One of the more striking occurrences in pedestrian dynamics is the evidence of spontaneous, self-organized motion. Pedestrians in very crowded open spaces tend to organize in lanes of uniform walking velocity (Fig. 5.9). Similarly, when facing a stationary crowd, pedestrians spontaneously self-organize in river-like streams (rivers of people) in order to cross it (Fig. 5.8). Why do pedestrians spontaneously organize themselves in this type of movement? How and by which mechanism do they evolve in space and time?

The constructal theory's answer to these questions is simple and direct. In line with the access-optimization principle, the optimal flow architecture will be the one that promotes the easiest flow of pedestrian. As described before, there are two locomotion modes for achieving motion: diffusion (slow or high resistivity) and channeling (fast or low resistivity). Diffusion is the preferred locomotion mode as long as it provides the faster pedestrian transport across the territory (e.g., for $L/\lambda < 1.2 - 0.5\lambda^{-1}$, i.e., for large inter-personal distances or low pedestrian densities). Otherwise, channeling becomes the most competitive transport mechanism. Channeling is faster and allows pedestrians to walk with very weak interpersonal interactions. This explains why moving pedestrians form lanes of uniform velocity when the density is high enough. The question is why do lanes of different velocity form? The answer to this is that a group of pedestrians

is often composed of many pedestrians with different walking velocities (e.g., young people walk faster than older people). Besides these, pedestrians follow others who are already moving. These factors are then responsible for differences of velocity between lanes.

The movement of pedestrians across stationary crowds (rivers of people) can be deduced from the constructal principle in a way similar to river basin structures (Bejan 2000, 2002). The crowd can be seen as the river basin and the space vacated by the crossing pedestrians as the eroded river bed (path of low resistance). Imagine one of the crossing pedestrians moving toward the stationary crowd. Its successor will see the "open space" vacated near by and will proceed to occupy it in order to be carried away. This means that pedestrians follow others who are already moving, giving rise to channeling networks of pedestrian to appear through the crowd. The lines formed by coalescence of many such paths are the river branches.

In crowds that panic, the streams of people of uniform walking velocity are destroyed because individuals do not know which the right way to escape is. They strive to go forward, thereby reducing interpersonal distances, inducing interpersonal contact (collision) or even loss of balance of other individuals.

5.7. Population Motion and Spread of Epidemics

Large-scale epidemic outbreaks have occurred through the centuries causing major surges in mortality (Anderson and May 1991; Cohn 2002; Suwandono et al. 2006), the worst being the bubonic plague (or Black Death) in the fourteenth century. Historians estimated that the Black Death wiped out a third of the European population in less than four years, no such large-scale outbreak has been reported since (Langer 1964). The last large-scale outbreak was the so-called Spanish Influenza epidemic of 1918–1919 (Oxford et al. 2005). It is estimated that about half of the people living worldwide became infected and 20 million died. An estimated 60,000 died in Portugal, 200,000 in the UK, more than 400,000 in France, and about 600,000 in the USA (Fig. 5.23).

Epidemic diseases still occur in many areas of our planet at a local scale (Barreto et al. 1994; Koopmans et al. 2004; Hsu et al. 2006). There can be little doubt that the improvement of healthcare, a greater vaccine manufacturing capacity, a development of hygiene habits, and an expanded surveillance reduced greatly the impact of an epidemic disease since the second-half of the twentieth century. Nevertheless, the widespread avian influenza outbreaks occurring nowadays throughout Asia show us that a global epidemic is still a possibility (Hsu et al. 2006).

In order to prevent epidemics and minimize disease transmission, it is essential that we are able to evaluate the epidemic spread mechanisms and capability. Models for spread of epidemics have existed since the early twentieth century. Perhaps the most well known are the SIR model (Kermack and McKendrick 1927) and the Noble's plague model (Noble 1974). In microparasite

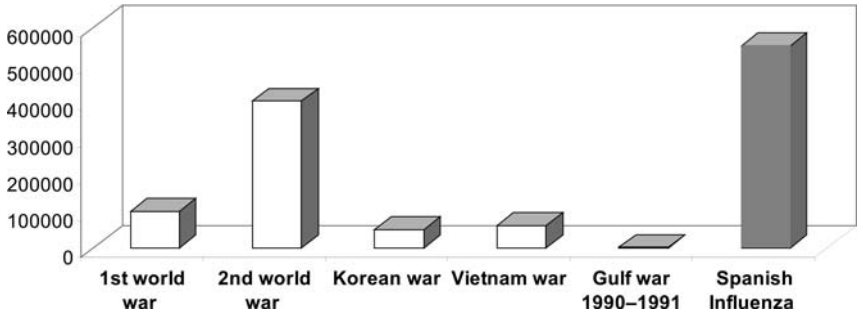

FIGURE 5.23. US military casualties in the wars of the twentieth century and America's deaths from Spanish influenza

infections (mainly viruses and bacteria), individuals are classified as susceptible (S), infected (I), or recovered (R). Susceptible individuals can catch the infection from contact with infected individuals, and the fraction of these individuals recovered is assumed to be immune to the disease. This leads to a set of balance equation that constitutes the SIR model. Extended versions of SIR model have been presented by Anderson and May (1992), Diekmann and Heesterbeek (2000), and Brauer and Castillo-Chavez (2001). On the other hand, the Noble's model considers that the spatial dispersal of individuals can be well approximated by a diffusion process, with the spread of epidemics being modeled as a diffusive–reactive phenomenon. This model was applied to the dynamics of bubonic plague as described throughout Europe in the fourteenth century. Since then reaction–diffusion models have been used to describe, among others, the spatial dynamics of rabies in fox (Kallen et al. 1985) and the Lyme disease transmission (Caraco et al. 2002). In this section we explore two main issues: the mechanics of epidemics propagation and the effect of population motion on the spread of epidemics.

5.7.1. Modeling the Spreading of an Epidemic

Consider two interacting populations of individuals—susceptible and infective. Transmission is the driving force due to which susceptible population becomes infective. The mass conservation of individuals S and I in a territory are governed by:

$$\frac{\partial S}{\partial t} = -\left(\frac{\partial}{\partial x} + \frac{\partial}{\partial y}\right) q_S \pm \psi_S \tag{5.37}$$

$$\frac{\partial I}{\partial t} = -\left(\frac{\partial}{\partial x} + \frac{\partial}{\partial y}\right) q_I \pm \psi_I \tag{5.38}$$

Here S and I are the density of susceptible and infective populations, q_S and q_I are the flux of susceptible and infected, and ψ_S and ψ_I are the sources/sinks

of susceptible and infected, respectively. To solve Eqs. (5.37) and (5.38) a representation of the fluxes q_S and q_I and sources/sinks ψ_S and ψ_I are required.

In ancient times, transporting commodities over any significant distances were an expensive and risky enterprise. Thus, travel and commerce was restricted mainly to local markets situated not far from home. Today, different modes of transportation (cars, trains, airplanes) deliver people in business and holidays to the most distant parts of the world in only a few hours. In the preceding section we have shown that diffusion and convection (channeling) are the regimes to distribute individuals through a territory (area). Therefore, we can consider that the flux of individuals is a convective–diffusive process, described generically by

$$q_S = -\left(\frac{\partial}{\partial x} + \frac{\partial}{\partial y}\right) D_S S + u_S S \tag{5.39}$$

$$q_I = -\left(\frac{\partial}{\partial x} + \frac{\partial}{\partial y}\right) D_I I + u_I I \tag{5.40}$$

where D_S and D_I are the diffusion coefficients of the susceptible and infective populations, respectively, and u_S and u_I are the velocities of the susceptible and infective populations, respectively. Combining relations (5.37) to (5.40) yields

$$\frac{\partial S}{\partial t} + \left(\frac{\partial}{\partial x} + \frac{\partial}{\partial y}\right) u_S S = \left(\frac{\partial^2}{\partial x^2} + \frac{\partial^2}{\partial y^2}\right) D_S S \pm \psi_S \tag{5.41}$$

$$\frac{\partial I}{\partial t} + \left(\frac{\partial}{\partial x} + \frac{\partial}{\partial y}\right) u_I I = \left(\frac{\partial^2}{\partial x^2} + \frac{\partial^2}{\partial y^2}\right) D_I I \pm \psi_I \tag{5.42}$$

The sources/sinks of susceptible and infective populations can be modeled based on the following assumptions: (i) natural births and deaths are proportional to the size of the susceptible population (Mena-Lorca and Hethcote 1992); (ii) the infective population has a disease-induced death that is proportional to its size (Nobel 1974); and (iii) the transmission from susceptible to infective is proportional to the size of the susceptible and infective populations (Nobel 1974). This then leads to:

$$\frac{\partial S}{\partial t} + \left(\frac{\partial}{\partial x} + \frac{\partial}{\partial y}\right) u_S S = \left(\frac{\partial^2}{\partial x^2} + \frac{\partial^2}{\partial y^2}\right) D_S S + \mu_{bdS} S - \sigma SI \tag{5.43}$$

$$\frac{\partial I}{\partial t} + \left(\frac{\partial}{\partial x} + \frac{\partial}{\partial y}\right) u_I I = \left(\frac{\partial^2}{\partial x^2} + \frac{\partial^2}{\partial y^2}\right) D_I I - \mu_{dI} I + \sigma SI \tag{5.44}$$

where μ_{bdS} is the net growth rate (e.g., rate of births minus the rate of natural deaths), μ_{dI} is the mortality rate induced by the disease, and σ is the disease transmission coefficient. Several time-scales can be obtained by applying scale analysis (Bejan 2000)

$$t_{dfi} = \frac{L_S^2}{D_S};\ t_{dfi} = \frac{L_I^2}{D_I} \tag{5.45}$$

$$t_{cv} = \frac{L_S}{u_S};\ t_{cv} = \frac{L_I}{u_I} \tag{5.46}$$

$$t_{\mu S} = \frac{1}{\mu_{dbS}};\ t_{\mu I} = \frac{1}{\mu_{dI}} \tag{5.47}$$

$$t_{\sigma S} = \frac{S}{I} t_{\sigma I};\ t_{\sigma I} = \frac{1}{\sigma S} \tag{5.48}$$

where t_{dif} and t_{cv} are the time scales associated with the diffusive and the convective populations motion (Section 5.3.1), $t_{\mu S}$ is the time scale associated with the births and life expectancy of the susceptible population, $t_{\mu I}$ is the life expectancy of an inflective, and $t_{\sigma I}$ is the contagious time of the disease.

Note that the diffusion and convective mechanisms only influence the spread of epidemic after it occurs but they do not play any role on whether the epidemic will occur. The time scale corresponding to the diffusive mode of travel is only smaller than the time scale corresponding to the convective mode if the territory length to access is smaller than D/u. Therefore, diffusion is the optimal travel regime to provide access to all locations while convection is optimal for providing access at large distances.

The growth rate of the susceptible population is strongly associated to $t_{\mu S}$ and $t_{\sigma I}$. There is a positive contribution to the growth of susceptibles since $t_{\mu S}$ is positive and the absolute value is smaller than $t_{\sigma I}$ (e.g., the ratio between μ_{bdS} and the density of infectives has to exceed the disease transmission coefficient). Furthermore, the development of the epidemic is strongly associated to $t_{\mu I}$ and $t_{\sigma I}$. When the life expectancy of an infective is much smaller than the contagious time, the disease tends to disappear. This topic will be detailed further in the next section.

5.7.2. Geotemporal Dynamics of Epidemics

The pattern of propagation of the Black Death and other plagues suggest a wave-like mechanism of propagation (Noble 1974). What are the conditions for the existence of waves? What kind of role do diffusive and convective regimes play on that? How do μ_{dI} and σ affect the propagation of the wave?

For the sake of simplicity, consider a one-dimensional wave traveling in a positive direction λ with a velocity c. Setting $S(x, t) = S(\Lambda)$ and $I(x, t) = I(\Lambda)$ with $\Lambda = \lambda - ct$, and substituting them into Eqs. (5.43) and (5.44) the following coupled differential equations are obtained:

$$\frac{\partial^2 S}{\partial \Lambda^2} + \frac{c - u_S}{D_S}\frac{\partial S}{\partial \Lambda} + \frac{\mu_{bdS} - \sigma I}{D_S} S = 0 \tag{5.49}$$

$$\frac{\partial^2 I}{\partial \Lambda^2} + \frac{c - u_I}{D_I}\frac{\partial I}{\partial \Lambda} + \frac{\sigma S - \mu_{dI}}{D_I} I = 0 \tag{5.50}$$

Since S and I cannot be negative, these equations may represent damped unforced harmonic oscillators under the following conditions: (i) $(c - u_S)/D_S \geq 0$,

$(c - u_I)/D_I \geq 0$ (damping factor) and (ii) $(\mu_{bdS} - \sigma I)/D_S \geq 0$, $(\sigma S - \mu_{dI})/D_I \geq 0$ (oscillatory factor). We are interested in the propagation of the infective population. According to Eq. (5.50), the natural frequency, ω_I, and the damped frequency, ω_{Id}, are

$$\omega_I = \left(\frac{\sigma S - \mu_{dI}}{D_I}\right)^{1/2} \tag{5.51}$$

$$\omega_{Id} = \left[\omega_I^2 - \frac{(c - u_I)^2}{4D_I^2}\right]^{1/2} \tag{5.52}$$

From these equations we note that the convective velocity is exclusively related to the damping factor while the diffusive process is related both with the damping and oscillatory factors. When the damping factor equals zero, $(c - u_I)/D_I = 0$, the system composed by the infective populations reduces to the case of a simple harmonic oscillator: continuous oscillation at the natural frequency ω_I. On the other hand, when $(c - u_I)/D_I > 0$, the system may or may not oscillate, depending on the relation between the damping factor and the natural frequency: If $\omega_I > (c - u_I)/2D_I$, the system is under damped conditions and exhibits transient behavior, oscillating at ω_{Id} with an amplitude that decays exponentially. When $(c - u_I)/2D_I \geq \omega_I$, there is no oscillatory behavior and the system returns smoothly to its equilibrium position. Thus, a wave-like solution can only exist when

$$c \geq u_I + 2\left[D_I(\sigma S - \mu_{dI})\right]^{1/2} \geq 0 \quad \text{and} \quad \sigma S \geq \mu_{dI} \tag{5.53}$$

This result has important implications that deserve to be analyzed. In the case of a wave-like solution, an increase of the diffusion coefficient D_I and velocity u_I implies waves with higher velocities. Besides these, the life expectancy of an inflective $(1/\mu_{dI})$ must be larger than the contagious time of the disease $(1/\sigma S)$. The last result has two consequences: (i) a wave-like solution implies a minimum critical value of the susceptible population density of $\sim \mu_{dI}/\sigma$, and (ii) there is a critical transmission coefficient from the infective to the susceptible population above which an epidemic wave occurs ($\sim \mu_{dI}/S$). Thus, low-populated territories and rapidly fatal diseases prevent the spread of infection. This explains why very deathly diseases, such as the Ebola virus, do not spread around the world: up to now these diseases show up in poorly populated and remote areas (e.g., σS is very small), and the life expectancy of the inflected population is very short.

The above results have important practical implications. If we reduce travel and commerce (e.g., diffusion and convection mechanisms), we also prevent the spread of the epidemic (an increase of diffusive and convective fluxes of infective population induce traveling waves with higher velocities). In territories having a susceptible population below the minimum critical density, a sudden influx of susceptible individuals may initiate an epidemic. On the other hand, when $S > \mu_{di}/\sigma$, a sudden outflow of susceptible (health) population or immunization of a part of individuals by medical intervention (vaccination, culling) reduces the

density of susceptible population and may prevent the spread of disease. Finally, by isolation of the infective population we are able to reduce the transmission coefficient σ and, if the critical transmission coefficient is not exceeded, there is no epidemic outbreak.

References

Anderson, R. M. and May, R. M. (1992) *Infectious Diseases of Humans*. Oxford University Press, London.

Ando, T., Ota, H. and Oki, T. (1988) Forecasting the flow of people. *Railw. Res. Rev.* **45**, 8–14.

Anthony, K. R. N. (1999) Coral suspension feeding on fine particulate matter. *J. Exp. Mar. Biol. Ecol.* **232**, 85–106.

Barreto, A., Aragon, M. and Epstein, R. (1994) Bubonic plague in Mozambique. *Lancet* **345**, 983–984.

Bégué, P. and Lorente, S. (2006) Migration vs. diffusion through porous media: time dependent scale analysis. *J. Porous Media* **7**, 637–650.

Bejan, A. (1997) *Advanced Engineering Thermodynamics*, 2nd edn, Wiley, New York.

Bejan, A. (1999) How nature takes shape: extensions of constructal theory to ducts, rivers, turbulence, cracks, dendritic crystals and spatial economics. *Int. J. Therm. Sci.* **38**, 653–663.

Bejan, A. (2000) *Shape and Structure, from Engineering to Nature*. Cambridge University Press, Cambridge, UK.

Bejan, A. (2002) Fundamentals of exergy analysis, entropy generation minimiza-tion, and the generation of flow architecture. *Int. J. Energy Res.* **26**, 545–565.

Bejan, A. (2005) The constructal law of organization in nature: tree-shaped flows and body size. *J. Exp. Biol.* **208**, 1677–1686.

Bejan, A. and Ledezma, G. A. (1998) Streets tree networks and urban growth: optimal geometry for quickest access between a finite-size volume and one point. *Physica A* **255**, 211–217.

Bejan, A. and Lorente, S. (2005) *La Loi Constructale*. L'Harmattan, Paris.

Bejan, A., Dincer, I., Lorente, S., Miguel, A. F. and Reis, A. H. (2004) *Porous and Complex Flow Structures in Modern Technologies*. Springer, New York.

Bejan, A., Lorente, S., Miguel, A. F. and Reis, A. H. (2006) *Along with Constructal Theory*, University of Lausanne, Faculty of Geosciences.

Ben-Jacob, E., Cohen, I., Shochet, O., Aronson, I., Levine, H. and Tsimering, L. (1995) Complex bacterial patterns. *Nature* **373**, 566–567.

Blue, V. and Adler, J. (1999) Bi-directional emergent fundamental pedestrian flows from cellular automata microsimulation. In A. Ceder (ed.), *Proc. Int. Symp. Traffic and Transportation Theory (ISTTT'99)*. Pergamon, Amsterdam, pp. 235–254.

Brauer, F. and Castillo-Chavez, C. (2001) *Mathematical Models in Population Biology and Epidemiology*. Springer, New York.

Caraco, T., Glavanakov, S., Chen, G., Flaherty, J. E., Ohsumi, T. K. and Szymanski, B. K. (2002) Stage-structured infection transmission and a spatial epidemic: A model for Lyme disease. *Am. Nat.* **160**, 348–359.

Cohn, S. K. (2002) The Black Death: end of a paradigm. *Am. Hist. Rev.* **107**, 703–738.

Diekmann, O. and Heesterbeek, J. A. P. (2000) *Mathematical Epidemiology of Infectious Diseases: Model Building, Analysis and Interpretation*. Wiley, New York.

Donald, I. and Canter, D. (1990) Behavioural aspects of the King's Cross disaster. In D. Canter (ed.), *Fires and Human Behaviour*. David Fulton, London, pp. 15–30.

Fang, Z., Lo, S. M. and Lu, J. A. (2003) On the relationship between crowd density and movement velocity. *Fire Saf. J.* **38**, 271–283.

Fruin, J. (1971) Pedestrian and planning design. Metropolitan Association of Urban Designers and Environmental Planners. Library of Congress catalogue number 70–159312.

Fukui, M. and Ishibashi, Y. (1999) Self-organized phase transitions in CA-models for pedestrians. *J. Phys. Soc. Japan* **8**, 2861–2863.

Gettling, A. V. (1998) *Rayleigh-Benard Convection: Structures and Dynamics*. World Scientific, Singapore.

Graat, E., Midden, C. and Bockholts, P. (1999) Complex evacuation: effects of motivation level and slope of stairs on emergency egress time in a sports stadium. *Saf. Sci.* **31**, 127–141.

Hankin, B. D. and Wright, R. A. (1958) Passenger flow in subways. *Oper. Res*. **9**, 81–88.

Heidemann, D. (1996) A queueing theory approach to speed–flow–density relationships, transportation and traffic theory. *Proc. 13th Int. Symp. Transport. Traffic Theory*, Lyon, pp. 14–26.

Helbing, D. (1992) A fluid-dynamic model for the movement of pedestrians. *Complex Syst.* **6**, 391–415.

Helbing, D. and Molnár, P. (1995) Social force model for pedestrian dynamics. *Phys. Rev. E* **51**, 4282–4286.

Helbing, D., Keltsch, J. and Molnár, P. (1997) Modeling the evolution of human trail systems. *Nature* **388**, 47–50.

Helbing, D., Schweitzer, F., Keltsch, J. and Molnár, P. (1997) Active walker model for the formation of human and animal trail systems. *Phys. Rev. E* **56**, 2527–2539.

Helbing, D. Molnár, P. Farkas, I. J. and Bolay, K. (2001) Self-organizing pedestrian movement. *Environ. Plan. Plan. Des.* **28**, 361–383.

Henderson, L. F. (1971) The statistics of crowd fluids. *Nature* **229**, 381–383.

Hodge, A., Robinson, D., Griffiths, B. S. and Fitter, A. H.(1999) Why plants bother: root proliferation results in increased nitrogen capture from an organic patch when two grasses compete. *Plant Cell Environ.* **22**, 811–820.

Hoogendoorn, S. and Bovy, P. H. L. (2000) Gas-kinetic modeling and simulation of pedestrian flows. *Transp. Res. Rec.* **1710**, 28–36.

Hoogendoorn, S., Bovy, P. and Daamen, W. (2002). Microscopic pedestrian way finding and dynamics modelling. In M. Schreckenberg and S. Sharma (eds.), *Pedestrian and Evacuation Dynamics*. Springer, New York, pp. 123–155.

Hsu, C. C., Chen, T., Chang, M. and Chang, Y. K. (2006) Confidence in controlling a SARS outbreak: Experiences of public health nurses in managing home quarantine measures in Taiwan. *Am. J. Infect. Control* **34**, 176–181.

Hughes, R. L. (2002) A continuum theory for the flow of pedestrians. *Transp. Res. B* **36**, 507–535.

Hughes, R. L. (2003) The flow of human crowds. *Annu. Rev. Fluid. Mech*. **35**, 169–182.

Hunter, K., Petty, M. D. and McKenzie, F. D. (2005) Experimental evaluation of the effect of varying levels of crowd behavior fidelity on the outcome of certain military scenarios. In Spring 2005 Simulation Interoperability Workshop, San Diego, CA.

Kaandorp, J. A. and Sloot, P. M. A. (2001) Morphological models of radiate accretive growth and the influence of hydrodynamics. *J. Theor. Biol.* **209**, 257–274.

Kallen, A., Arcuri, P. and Murray, J. D. (1985) A simple model for the spatial spread and control of rabies. *J. Theor. Biol.* **116**, 377–394.

Kermack, W. O. and McKendrick, A. G. (1927) A contribution to the mathematical theory of epidemics.*Proc. R. Soc. London A* **115**, 700–721.

Koopmans, M., Wilbrink, B., Conyn, M., Natrop, G., van der Nat. H., Vennema, H., Meijer, A., van Steenbergen, J., Fouchier, R., Osterhaus, A. and Bosman, A. (2004) Transmission of H7N7 avian influenza A virus to human beings during a large outbreak in commercial poultry farms in the Netherlands. *Lancet* **363**, 587–593.

Langer, W. L. (1964) The black death. *Scient. Am*. **210**, 114–121.

Langston, P. A., Masling, R. and Asmar, B. N. (2006) Crowd dynamics discrete element multi-circle model, *Saf. Sci.* **44**, 395–417

Mena-Lorca, J. and Hethcote, H. (1992) Dynamic models of infection diseases as regulator of population sizes. *J. Math. Biol.* **30**, 693–716.

Merks, R., Hoekstra, A., Kaandorp, J. and Sloot, P. (2003) Models of coral growth: spontaneous branching, compactification and the Laplacian growth assumption.*J. Theor. Biol*. **224**, 153–166.

Miguel, A. F. (2004) Dendritic growth: classical models and constructal analysis. In R. Rosa, A.H. Reis, A.F. Miguel (eds.) *Bejan's Constructal Theory of Shape and Structure*. CGE-UE, Evora, pp. 75–93

Miguel, A. F. (2006) Constructal pattern formation in stony corals, bacterial colonies and plant roots under different hydrodynamics conditions. *J. Theor. Biol.* **242**, 954–961

Muramatsu, M., Irie, T. and Nagatani, T. (1999) Jamming transition in pedestrian counter flow. *Physica A* **267**, 487–498.

Navin, P. D. and Wheeler, R. J. (1969) Pedestrian flow characteristics. *Traffic Eng.* **39**, 31–36.

Nelson, H. E. and Maclennan, H. A. (1995) Emergency movement. *The SFPE Handbook of Fire Protection Engineering*, 2nd edn, NFPA, Quincy, MA.

Noble, J. V. (1974) Geographic and temporal development of plagues. *Nature* **250**, 276–279.

Older, S. J. (1968) Movement of pedestrians on footways in shopping streets. *Traffic Eng. Control* **10**, 160–163.

Oxford, J. S., Lambkin. R., Sefton, A., Daniels, R., Elliot, A., Brown, R. and Gill, D. (2005) A hypothesis: the conjunction of soldiers, gas, pigs, ducks, geese and horses in Northern France during the Great War provided the conditions for the emergence of the "Spanish" influenza pandemic of 1918–1919. *Vaccine* **23**, 940–945.

Predtechenskii, V.M. and Milinski, A. I. (1969) *Planning for Foot Traffic Flow in Buildings*. Stroiizdat Publishers, Moscow.

Reis, A. H., Miguel. A. F. and Aydin, M. (2004) Constructal theory of flow architecture of the lungs. *Med. Phys.* **31**, 1135–1140.

Reis, A. H. (2006a) Constructal view of scaling laws of river basins. *Geomorphology* **78**, 201–206.

Reis, A. H. (2006b) Constructal theory: from engineering to physics, and how flow systems develop shape and structure. *Appl. Mech. Rev*. **59**, 269–282.

Reis, A. H. and Miguel, A. F. (2006) Constructal theory and flow architectures in living systems. *J. Thermal Sci.* **10**, 57–64.

Reynolds, C. W. (1987) Flocks, herds, and schools: a distributed behavioral model. *Comput. Graphics* **21**, 25–34.

Robinson, D. (1994) The responses of plants to non-uniform supplies of nutrients. *New Phytol.* **127**, 635–674.

Rosa, R., Reis, A. H. and Miguel, A. F. (2004) *Bejan's Constructal Theory of Shape and Structure*. Geophysics Center of Evora, University of Evora, Portugal.

Sandahl, J. and Percivall, M. (1972) A pedestrian traffic model for town centers. *Traffic Q.* **26**, 359–372.

Schweitzer, F. (1997) *Self-organization of Complex Structures: From Individual to Collective Dynamics*. Gordon and Breach, London.

Sebens, K. P., Witting, J. and Helmuth, B. (1997) Effects of water flow and branch spacing on particle capture by the reef coral Madracis mirabilis (Duchassaing and Michelotti). *J. Exp. Mar. Biol. Ecol*. **211**, 1–28.

Smith, R. A. and Dickie, J. F. (1993) *Engineering for Crowd Safety*. Elsevier, Amsterdam.

Suwandono, A., Kosasih, H., Nurhayati, H., Kusriastuti, R., Harun, S., Maroef, C., Wuryadi, S., Herianto, B., Yuwono, D., Porter, K. R., Beckett, C. G. and Blair, P. J. (2006) Four dengue virus serotypes found circulating during an outbreak of dengue fever and dengue haemorrhagic fever in Jakarta, Indonesia, during 2004. *Trans. R. Soc. Trop. Med. Hyg.* **100**, 855–862.

Thaler, P. and Pages L. (1998) Modeling the influence of assimilate availability on root growth and architecture. *Plant Soil* **201**, 307–320.

Thar, R. and Kühl, M. (2005) Complex pattern formation of marine gradient bacteria explained by a simple computer model. *FEMS Microbiol. Lett.* **246**, 75–79.

The Green Guide (1997) *Guide to Safety at Sports Grounds*, 4th edn, HMSO, London.

Thompson, P. A. and Marchant, E. W. (1995) A computer model for the evacuation of large building populations. *Fire Saf. J*. **24**, 131–148.

Timmermans, H., van der Hagen, X. and Borgers, A. (1992) Transportation systems, retail environments and pedestrian trip chaining behaviour: modelling issues and applications. *Transport. Res. B: Methodological* **26**, 45–59.

Togawa, K. (1955) Study on fire escape based on the observations of multitude currents. Report No. 4. Building Research Institute, Ministry of Construction, Japan.

TRB (1985) Pedestrians. In *Highway Capacity Manual*, special report 209, Transportation Research Board, Washington, DC, Chapter 13.

Vandaele, N., Woensel, T. V. and Verbruggen, A. (2000) A queueing based traffic flow model. *Transport. Res. D* **5**, 121–135.